Macromolecular Bioscience
www.mbs-journal.de

Visible Light Cross-Linking of Gelatin Hydrogels Offers an Enhanced Cell Microenvironment with Improved Light Penetration Depth

Khoon S. Lim, Barbara J. Klotz, Gabriella C. J. Lindberg, Ferry P. W. Melchels, Gary J. Hooper, Jos Malda, Debby Gawlitta, and Tim B. F. Woodfield**

In this study, the cyto-compatibility and cellular functionality of cell-laden gelatin-methacryloyl (Gel-MA) hydrogels fabricated using a set of photo-initiators which absorb in 400–450 nm of the visible light range are investigated. Gel-MA hydrogels cross-linked using ruthenium (Ru) and sodium persulfate (SPS), are characterized to have comparable physico-mechanical properties as Gel-MA gels photo-polymerized using more conventionally adopted photo-initiators, such as 1-[4-(2-hydroxyethoxy)-phenyl]-2-hydroxy-2-methyl-1-propan-1-one (Irgacure 2959) and lithium phenyl(2,4,6-trimethylbenzoyl) phosphinate (LAP). It is demonstrated that the Ru/SPS system has a less adverse effect on the viability and metabolic activity of human articular chondrocytes encapsulated in Gel-MA hydrogels for up to 35 days. Furthermore, cell-laden constructs cross-linked using the Ru/SPS system have significantly higher glycosaminoglycan content and re-differentiation capacity as compared to cells encapsulated using I2959 and LAP. Moreover, the Ru/SPS system offers significantly greater light penetration depth as compared to the I2959 system, allowing thick (10 mm) Gel-MA hydrogels to be fabricated with homogenous cross-linking density throughout the construct. These results demonstrate the considerable advantages of the Ru/SPS system over traditional UV polymerizing systems in terms of clinical relevance and practicability for applications such as cell encapsulation, biofabrication, and in situ cross-linking of injectable hydrogels.

1. Introduction

In recent years, scaffold-based strategies adopting hydrogels as biomaterials for tissue engineering have received significant attention and offer a number of advantages due to their highly hydrated polymeric network and their structural similarity to native extracellular matrix.[1] Among these, photo-polymerizable gelatin hydrogels are especially attractive as they offer the ability for spatial and temporal control over the polymerization process. Additionally, the reaction can be performed at room or

Dr. K. S. Lim, Dr. G. C. J. Lindberg, Prof. G. J. Hooper, Prof. T. B. F. Woodfield
Christchurch Regenerative Medicine and Tissue Engineering (CReaTE) Group
Department of Orthopaedic Surgery and Musculoskeletal Medicine
University of Otago Christchurch
Christchurch 8011, New Zealand
E-mail: khoon.lim@otago.ac.nz; tim.woodfield@otago.ac.nz

Dr. K. S. Lim, Dr. G. C. J. Lindberg, Prof. T. B. F. Woodfield
Medical Technologies Centre of Research Excellence
Auckland 1010, New Zealand

Dr. K. S. Lim, Prof. T. B. F. Woodfield
Maurice Wilkins Centre for Molecular Biodiscovery
Auckland 1010, New Zealand

B. J. Klotz, Prof. D. Gawlitta
Department of Oral and Maxillofacial Surgery & Special Dental Care
University Medical Center Utrecht
PO 85500, Utrecht GA 3508, The Netherlands

Prof. J. Malda
Regenerative Medicine Center Utrecht
PO 85500, Utrecht GA 3508, The Netherlands

Prof. F. P. W. Melchels
Institute of Biological Chemistry, Biophysics and Bioengineering
School of Engineering and Physical Sciences
Heriot-Watt University
Edinburgh, EH14 4AS, United Kingdom

Prof. J. Malda
Department of Orthopaedics
University Medical Center Utrecht
PO 85500, Utrecht GA 3508, The Netherlands

Prof. J. Malda
Department of Equine Sciences
Faculty of Veterinary Medicine
Utrecht University
Yalelaan 112, Utrecht CM 3584, The Netherlands

The ORCID identification number(s) for the author(s) of this article can be found under https://doi.org/10.1002/mabi.201900098.

DOI: 10.1002/mabi.201900098

physiological temperature, with fast curing rates and minimal heat generation.[2,3]

In general, the photo-polymerization process requires grafting of functional photo-labile moieties, such as methacryloyl (methacrylamides and methacrylates), tyramine, or styrene to gelatin.[4–10] Among these different photo-crosslinkable gelatin materials, gelatin-methacryloyl (Gel-MA) has emerged as a promising biomaterial due to the tailorable physical properties (cross-linking density, swelling, and stiffness) depending on the degree of methacryloyl substitution and the initial macromer concentration, thereby making it a versatile platform for various tissue engineering applications.[4,11] To date, the most commonly used photo-initiator to cross-link Gel-MA is 1-[4-(2-hydroxyethoxy)-phenyl]-2-hydroxy-2-methyl-1-propan-1-one, which is also known as Irgacure 2959 (I2959).[12,13] When exposed to ultraviolet (UV) light, Gel-MA undergoes cross-linking through chain-growth radical polymerization. Here, the I2959 molecules absorb photons of light and dissociate into radicals, which then propagate through the methacryloyl groups, forming covalent kinetic chains to hold the polymer chains together (**Figure 1**A).[13]

However, one major drawback of using I2959 is that it requires ultraviolet (UV) light for photo-excitation, which can potentially cause cellular DNA and tissue damage.[14–16] For example, previous studies conducted by Dahle et al. demonstrated that both UVA (320–400 nm) and UVB (290–320 nm) radiation can induce chromosomal, as well as genetic instability in mammalian cells.[17,18] Furthermore, Lavker et al. reported that repetitive exposure of human skin to low dose of UVA resulted in dermal alternations such as inflammation and lysozyme deposition.[19] UV light can also react with oxygen in the environment, forming reactive oxygen species (ROS), such as the superoxide radical ($O_2^{\cdot\cdot}$), hydroxyl radical ($OH^{\cdot}$), singlet oxygen ($^1O_2$), and ozone (O_3), which have also been shown to cause oxidative damage to DNA.[19,20] Additionally, for in vivo injectable hydrogel applications, UV light has been previously reported to have limited light penetration depth and can be attenuated by the native tissue.[21,22] Elisseeff et al. showed that transmittance of UVA through human skin was significantly reduced, where visible light photo-initiating systems were more efficient for transdermal polymerization.[23] Therefore, the development and cell-related characterization of alternative photo-polymerization systems that operate in the visible light (400–700 nm) spectrum may offer significant advantages for tissue engineering applications such as cell delivery or as space-fillers post augmentation, compared to more common UV photo-polymerization.

To date, a number of visible light photo-initiating systems have been investigated to fabricate cell-laden Gel-MA hydrogels, and include: camphorquinone,[24,25] fluorescein,[24] rose bengal,[26] riboflavin,[24] lithium phenyl-2,4,6-trimethylbenzoylphosphinate (LAP),[27,28] and eosin Y.[29] In particular, LAP behaves very similarly to I2959, both being type 1 photo-initiators that undergo unimolecular bond cleavage to generate free

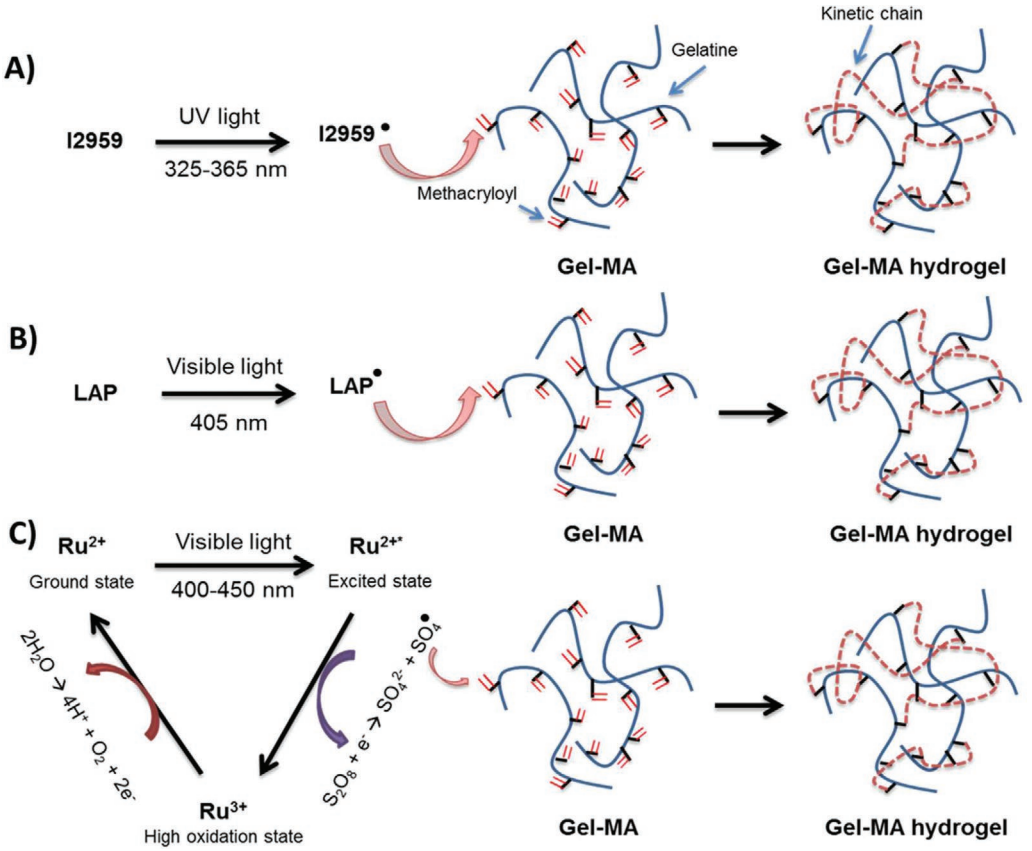

Figure 1. Schematic of the Gel-MA cross-linking process using A) UV light and I2959; B) visible light and LAP; C) visible light and Ru/SPS.

radicals to facilitate polymerization (Figure 1B).[14,27] However, LAP has limited molar absorptivity in a narrow visible light range ($\varepsilon \approx 30$ M^{-1} cm^{-1} at 405 nm), resulting in the need of using high concentrations to fabricate hydrogels.[14,27] On the other hand, although eosin-Y has a much higher molar absorptivity ($\varepsilon \approx 100\,000$ M^{-1} cm^{-1} at 525 nm), it often requires the presence of both a co-initiator (triethanolamine) and a co-monomer (*N*-vinylpyrrolidone or *N*-vinylcaprolactam) to facilitate methacryloyl-based photo-polymerization.[30–33] In contrast, another emerging visible light–initiating system, consisting of a ruthenium (Ru)-based transition metal complex ($\varepsilon \approx 14\,600$ M^{-1} cm^{-1} at 450 nm) and sodium persulfate (SPS), has shown potential for tissue engineering applications.[34–37] When irradiated with visible light, the photo-excited Ru^{2+} oxidizes into Ru^{3+} by donating electrons to SPS (Figure 1B). After accepting electrons, SPS dissociates into sulfate anions and sulfate radicals (Figure 1B). These radicals are subsequently able to cross-link Gel-MA by propagating through the methacryloyl groups.[38,39] However, the cellular functionality such as cell differentiation and tissue formation in cell-laden constructs photo-crosslinked using this Ru/SPS visible light system has not been investigated. Moreover, the feasibility of this visible light photo-initiating system to allow fabrication of large and thick constructs for in situ photo-curing has also not been demonstrated.

Therefore, the aim of this study was to assess cyto-compatibility and cell functionality of cell-laden Gel-MA hydrogels fabricated using the Ru/SPS visible light photo-initiating system. We describe herein the systematic characterization of physical properties of the visible light cross-linked Gel-MA hydrogels over a range of photo-initiator concentrations and irradiation conditions, compared to the two conventional and most commonly adopted systems, UV + I2959 and Vis + LAP. With clinical translation of this system in mind, we also evaluated the light penetration depth of the Ru/SPS system to assess the feasibility of developing thick, fully cross-linked tissue engineered constructs while maximizing cell viability. Given that one of the potential applications of cell-encapsulated visible light cross-linked Gel-MA hydrogels is in cartilage tissue engineering, we investigated the in vitro re-differentiation capacity of expanded human articular chondrocytes as a clinically relevant cell source for further characterization of the Ru/SPS system.

2. Experimental Section

2.1. Materials

Gelatin (porcine skin, type A, 300 g Bloom strength), phosphate buffered saline (PBS), methacrylic anhydride, cellulose dialysis membrane (14 kDa molecular weight cut-off), L-ascorbic acid-2-phosphate (AsAp), tris(2,2-bipyridyl)dichlororuthenium(II) hexahydrate (Ru), SPS, calcein-AM, propidium iodide (PI), proteinase K, dimethyl-methylene blue (DMMB), ethylenediaminetetraacetic acid disodium salt dihydrate (Di-sodium-EDTA), sodium chloride (NaCl), hyaluronidase, ITS+1, dexamethasone, hydrochloric acid (37%), sodium hydroxide (NaOH), chondroitin sulfate A (CS-A), and L-proline were purchased from Sigma-Aldrich (Missouri, USA). 1-[4-(2-hydroxyethoxy)-phenyl]-2-hydroxy-2-methyl-1-propan-1-one (Irgacure 2959) was a gift from BASF (Ludwigshafen, Germany). Collagenase type II was purchased from Worthington Biochemical Corporation (Lakewood, USA). Lithium phenyl-2,4,6-trimethylbenzoylphosphinate (LAP) was purchased from Toyo Chemical Industry (Tokyo, Japan). Dulbecco's Modified Eagle's Medium (DMEM) high glucose, 4-(2-hydroxyethyl)-1-piperazine-ethanesulfonic acid (HEPES), Gibco non-essential amino acids (NEAA), fetal calf serum (FCS), 0.25% trypsin/EDTA, penicillin–streptomycin (PS, 10 000 U mL^{-1}), AlamarBlue reagent, bovine serum albumin (BSA), goat-anti-mouse secondary antibody (Alexa Fluor 488), F-actin rhodamine phalloidin (Alexa Fluor 594 Phalloidin), 4,6-diamidino-2-phenylindole (D1306, DAPI), and the CyQUANT cell proliferation assay kit were purchased from ThermoFisher Scientific (Auckland, New Zealand). Medical grade silicone sheets were obtained from BioPlexus (Ventura, USA). Cell strainers (100 μm) were purchased from BD Biosciences (Auckland, New Zealand). Di-sodium hydrogen phosphate (Na_2HPO_4) and acetic acid (glacial, 100%) were ordered from Merck Millipore (Darmstadt, Germany). Optimal cutting temperature compound (OCT) was obtained from VWR International (Auckland, New Zealand). Transforming growth factor β 1 (TGFβ-1) was purchased from R&D systems, Minneapolis, USA. Primary antibodies for collagen II (II-II6B3-C) were purchased from DSHB (Iowa City, USA). Primary antibodies for collagen I (Ab34710) and aggrecan (Ab3773) were obtained from Abcam (Melbourne, Australia).

2.2. Synthesis of Gelatin-Methacryloyl

Gelatin was dissolved in PBS at a 10 wt% concentration, with 0.6 g of methacrylic anhydride per gram of gelatin added to the solution and left to react for 1 h at 50 °C under constant stirring.[4] This was followed by dialysis against deionized water to remove unreacted methacrylic anhydride. The purified Gel-MA solution was filtered through a 0.22 μm sterile filter and then lyophilized under sterile conditions. The degree of methacryloyl substitution was quantified to be 60% (data not shown) using ^{1}H-proton nuclear magnetic resonance spectroscopy (Bruker Avance 400 MHz).

2.3. Fabrication of Gel-MA Hydrogels

Dried sterile Gel-MA (10 wt%) was dissolved in PBS at 37 °C and left to cool overnight at RT. Prior to cross-linking, the Gel-MA solution was heated to 37 °C, then Ru and SPS were added, scooped into the silicon molds (5 mm diameter x 1 mm thickness) on a glass slide, and sandwiched with a cover slip. The samples were then irradiated (20 cm distance from light source for all experiments) under light (OmniCure S1500, Excelitas Technologies). The light was irradiated through a light filter (Rosco IR/UV filter) where only light of wavelength 400–450 nm and final intensity of 30 mW cm^{-2} was allowed to pass through. A variety of initiator concentrations (0.1/1, 0.2/2, and 0.3/3 of Ru/SPS [mM/mM]) and exposure times (0.5, 1, 3, 5, 10, and 15 min) were studied to optimize the irradiation conditions. Gel-MA hydrogels fabricated using Vis (intensity = 30 mW cm^{-2}, 400–450 nm) + 0.05 wt% LAP, UV

(intensity = 30 mW cm^{-2}, 300–400 nm) + 0.05 wt% I2959, and a variety of exposure times (0.5, 1, 3, 5, 10, and 15 min) were used as controls.

2.3.1. Swelling and Mass Loss Analysis

All samples were weighed for the initial wet mass ($m_{\text{initial,t0}}$) after cross-linking, and three samples were lyophilized immediately to obtain their dry weights ($m_{\text{dry,t0}}$). The actual macromer fraction was calculated based on the equation below.

$$\text{Actual macromer fraction} = \frac{m_{\text{dry,t=0}}}{m_{\text{initial,t=0}}} \tag{1}$$

These samples were then submerged in a bath of PBS and incubated at 37 °C. Samples were removed from the incubator after 1 day, blotted dry, and weighed (m_{swollen}). The swollen samples were then freeze-dried and weighed again (m_{dry}). The sol fraction and mass swelling ratio (q) were calculated as follows:

$$m_{\text{initial,dry}} = m_{\text{initial}} \times \text{actual macromer fraction} \tag{2}$$

$$\text{Sol fraction} = \frac{m_{\text{initial,dry}} - m_{\text{dry}}}{m_{\text{initial,dry}}} \times 100\% \tag{3}$$

$$q = \frac{m_{\text{swollen}}}{m_{\text{dry}}} \tag{4}$$

2.3.2. Compression Testing

The stiffness of the fabricated hydrogels was measured at room temperature using a dynamic mechanical analyzer (TA instruments, DMA 2980). Unconfined compression testing was performed at 30% strain per minute (5 mm diameter × 2 mm thickness), and the corresponding force was measured at a sampling frequency of 1.67 Hz. Sample diameter was measured using vernier calipers, and the compressive modulus was calculated from the slope of the linear region (10–15% strain range) of the stress–strain curves as previously reported.[7]

2.4. Cartilage Excision, Chondrocyte Isolation, and Expansion

Healthy human articular cartilage was harvested following ethics approval (New Zealand Health and Disability Ethics Committee—URB/07/04/014) from a consenting 28-year-old female patient undergoing ligament reconstruction of the knee. The cartilage was diced into 1–2 mm cubes and digested overnight at 37 °C with 0.15% w/v collagenase type II in basic chondrocyte medium (DMEM high glucose medium supplemented with 10% FCS, 10 mM HEPES, 0.2 mM L-ascorbic acid-2-phosphate, 0.4 mM L-proline, and 1% penicillin/streptomycin). The resulting suspension was filtered through a 100-µm cell strainer to exclude the undigested tissue and centrifuged at 700 *g* for 4 min. Isolated human articular chondrocytes (HACs) were cultured in basic chondrocyte medium and expanded at 37 °C in a humidified 5% CO_2/95% air incubator. Media was refreshed twice per week.

2.5. HAC Encapsulation in Gel-MA Hydrogels

Expanded HACs at P2 were trypsinized and suspended in basic chondrocyte medium. The cell suspension was added to the macromer solution containing sterile filtered initiators to give a final concentration of 5×10^6 HACs per milliliter. The cell-laden gels were then fabricated as outlined previously in Section 2.3. Samples were then irradiated for 15 min at an intensity of 30 mW cm^{-2} for both UV and visible light, where initiator concentrations were kept at 0.05 wt% I2959, 0.05 wt% LAP, or 0.2/2 (mM/mM) Ru/SPS respective to the light source. Constructs were cultured in chondrogenic differentiation media (Dulbecco's DMEM high glucose supplemented with 0.4 mM L-proline, 10 mM HEPES, 0.1 mM NEAA, 100 U mL^{-1} penicillin, 0.1 mg mL^{-1} streptomycin, 0.2 mM AsAp, 1 × ITS+1 premix, 1.25 mg mL^{-1} BSA, 10 nM dexamethasone, and 10 ng mL^{-1} TGFβ-1). Live/dead, AlamarBlue, glycosaminoglycan (GAG), and DNA assays were performed on the samples after 1, 21, 35 days in culture, as described below.

2.6. Live/Dead Assay

Harvested samples were washed with PBS, then stained with 1 µg mL^{-1} of calcein-AM and 1 µg mL^{-1} of PI for 10 min. Live cells stained green whereas dead cell nuclei stained red. After staining, the gels were washed with PBS thrice before imaging them, using a fluorescence microscope (Zeiss Axio Imager Z1). The number of live and dead cells was quantified using the ImageJ software (Bio-Formats plugin), and the cell viability was calculated using the equation below.

$$\text{Viability}\,(\%) = \frac{\text{Number of live cells}}{\text{Number of live cells + dead cells}} \times 100\% \tag{5}$$

2.7. AlamarBlue Assay

An AlamarBlue assay was performed to determine the metabolic activity of cells according to the manufacturer's protocol. Samples were incubated in basic chondrocyte medium containing 10% v/v AlamarBlue reagent for 24 h. The AlamarBlue reagent is reduced from blue to red/pink color by metabolically active cells. The reduction in AlamarBlue reagent was calculated after measuring the absorbance at 570 nm, using 600 nm as a reference wavelength (Fluostar Galaxy BMG Labtechnology).

2.8. Glycosaminoglycan and DNA Assay

GAG and DNA content were measured as described previously.[3,40] Briefly, cell-laden Gel-MA samples were digested overnight in 200 µL of 1 mg mL^{-1} proteinase-K solution at 56 °C. In order to quantify the amount of GAG retained in the gel, the digested samples were reacted with DMMB dye. The

absorbance was then measured on a plate reader at 520 nm (Fluostar Galaxy BMG Labtechnology). GAG content was calculated from a standard curve constructed using known concentrations of chondroitin sulfate-A. The DNA content in the gels was measured using a CyQUANT kit. Following digestion, cells were lysed and RNA degraded using the provided lysis buffer with RNase A (1.35 KU mL^{-1}) added for 1 h at RT. GR-dye solution was then added to the samples, incubated at RT for 15 min, then the fluorescence was measured (Fluostar Galaxy BMG Labtechnology). A standard curve was constructed using the DNA provided in the kit.

2.9. Immunofluorescence Histological Examination

The cell-laden constructs were fixed in 10% formalin for 1 h at RT and washed in PBS supplemented with 0.1 M glycine. For histological evaluation, the samples were embedded in OCT, then cryo-sectioned (30 μm thick sections).[8,32] Sections were incubated in 0.1 wt% hyaluronidase for 30 min at RT, washed with PBS, and blocked with 2 wt% BSA in PBS for 1 h at RT. Primary antibodies for collagen type I (1:200, rabbit), collagen type II (1:200, mouse), or aggrecan (1:300, mouse) were diluted in blocking buffer and applied overnight at 4 °C. Samples were washed thrice in blocking buffer for 10 min each, followed by incubation with a goat-anti-mouse (Alexa Fluor 488) and donkey-anti-rabbit (Alexa Fluor 594) secondary antibodies, diluted in blocking buffer (1:400), in the dark for 1 h at RT. For the last 10 min of the incubation, 4′,6-diamidino-2-phenylindole dihydrochloride (DAPI, 1:1000 dilution) was added. Lastly, constructs were washed thrice in PBS and visualized using the Zeiss Axioimager Z1 microscope.

2.10. Gene Expression

Samples cultured for 1 week were collected, digested in 10 mg mL^{-1} proteinase K solution at 55 °C for 30 min, incubated with 1 mL TRIzol reagent for 5 min at RT followed by RNA isolation in accordance with the manufacturer's guidelines. In brief, 200 μL of chloroform was vigorously mixed with the samples, followed with 3 min RT incubation and 15 min centrifugation at 12 000 g. The aqueous phase containing the RNA was transferred to tubes containing 500 μL isopropanol, then incubated at RT for 20 min, followed by centrifugation for 10 min at 12 000 *g*. The RNA pellet was washed twice in cold 70% ethanol and re-suspended in RNase-free water. Ambion DNA-free DNase Treatment was further used to remove any contaminating DNA according to manufacturer's instructions. Total RNA yield was determined using a spectrophotometer (Thermo Scientific, NanoDrop 8000) and the integrity was validated electrophoretically (Agilent Technologies, 2200 TapeStation). Total RNA, 300 ng per sample, was reverse transcribed into complementary DNA (cDNA) using TaqManTM first strand synthesis. Polymerase chain reaction (PCR) was then performed using an iCycler quantitative real-time PCR (qRT-PCR) machine (Roche, LightCycler480 II), SYBRGreen and primers (Sigma-Aldrich, KiCqStart SYBR Green Primers). The specific genes of interest were collagen type IA1 (GenBank accession no. NM_000088), collagen type IIA1 (GenBank accession no. NM_001844) and aggrecan (GenBank accession no. NM_001135). Glyceraldehyde-3-phosphate dehydrogenase (GAPDH, Sigma-Aldrich, GenBank accession no. NM_002046) was selected as housekeeping gene. Each sample was run in duplicate, and the threshold cycle and primer efficiency were analyzed, where the geometric mean of the reference gene (GAPDH) was used to calculate the normalized mRNA expression of each target gene.

2.11. Light Penetration Depth Study

Gel-MA macromers, 10 wt%, were prepared as outlined above in Section 2.3. Prior to cross-linking, Ru and SPS were added to the Gel-MA solution for a final concentration of 0.2/2 (mM/mM) Ru/SPS, pipetted into silicon molds (5 mm diameter × 10 mm thickness) on a glass slide, and sandwiched with a cover slip. The samples were then irradiated under light (Omni-Cure S1500, Excelitas Technologies) for 15 min through a light filter (Rosco IR/UV filter) where only light of 400–450 nm wavelength and final intensity of 30 mW cm^{-2} was allowed to pass through. Gel-MA hydrogels fabricated using UV light (intensity = 30 mW cm^{-2}, 300–400 nm); 0.05 wt% I2959 and 15 min of exposure time were used as controls. The fabricated hydrogels were then carefully removed from the mold and sliced into five 2-mm thick sections and marked as regions (i to v) relative to the depth from the irradiation source. The sections were then subjected to mass loss and swelling studies, as outlined in Section 2.3.1. A similar setup was also adopted to fabricate HAC-laden constructs, with subsequent live/dead analysis (Section 2.7) performed to evaluate cell viability within each of the five regions (i to v) relative to the depth from the irradiation source.

2.12. Transdermal Polymerization and In Vivo Subcutaneous Implantation

Gel-MA hydrogels fabricated using either UV + I2959 or Vis + Ru/SPS were implanted subcutaneously in BALB/C mice as per ethics approval C3/16. All hydrogel macromer components were sterile filtered prior to usage; the samples were cross-linked sterilely in a laminar flow hood and incubated in sterile PBS overnight prior to implantation. Female BALB/C mice were anaesthetized using inhalational isoflurane. After shaving and disinfection, subcutaneous pockets of approximately 10 mm deep were made by blunt dissection in a ventral direction from the incision down the side of the mouse in both directions. The pre-fabricated sterile Gel-MA hydrogels were then inserted into the base of the subcutaneous pocket, and the incision was closed using sutures and surgical glue. After 14 days, the mice were sacrificed, and the implants with surrounding tissue and underlying muscle were carefully dissected from the subcutaneous site and fixed in 4% v/v phosphate buffered formalin for at least 1 day at 4 °C. The harvested samples were then cryo-sectioned (30 μm sections) and stained with hematoxylin (H) and eosin (E). For imitation of transdermal polymerization, the mice were shaven after being sacrificed, the

skin from the dorsal region was harvested, and tissue hydration was maintained in a saline bath. Gel-MA macromer solution, 10 wt%, with either 0.2/2 (mM/mM) Ru/SPS or 0.05 wt% I2959 was pipetted into silicon molds (5 mm diameter × 10 mm thickness) on a glass slide and sandwiched with a cover slip. The harvested skin samples were then placed on top of the samples, and light (OmniCure S1500, Excelitas Technologies) was allowed to irradiate through the skin for 15 min to cross-link the samples. A final intensity of 30 mW cm^{-2} was used for both the UV and visible light systems. Hydrogels fabricated with the same conditions without being covered by skin were used as controls. The fabricated hydrogels were then carefully removed from the mold and subjected to mass loss analysis as outlined in Section 2.3.1.

2.13. Statistical Analysis

All results were analyzed using a two-way ANOVA with post-hoc Tukey's multiple comparisons tests unless stated. Data for mass loss and swelling studies were analyzed using a one-way ANOVA. The models were constructed using GraphPad Prism (GraphPad Software, version 6). Samples in each study were all prepared in triplicate, and all studies were repeated thrice ($n = 3$). A $p < 0.05$ was considered as statistically significant.

3. Results

3.1. Fabrication of Gel-MA Hydrogels

3.1.1. Optimization of Initiator Concentrations

Gel-MA hydrogels were successfully fabricated using the Ru/SPS photo-initiator system in the 400–450 nm visible light range. Optimization of the irradiation conditions required to fabricate Gel-MA hydrogels was investigated by examining a range of initiator concentrations while keeping the light intensity constant at 30 mW cm^{-2}. This was based on previously reported data indicating this light intensity as optimal for protein–protein cross-linking.[41,42] The cross-linking efficiency was measured by the sol fraction (Equation (3)), which is defined as the weight fraction of polymer chains that are not covalently bound to the hydrogel network after photo-polymerization.[1,43,44] It was observed that at 0.1/1 Ru/SPS (mM/mM), a minimum of 5 min exposure time was required to fabricate stable hydrogels, with resultant sol fraction of approximately 35–42% (**Figure 2**A). Increasing the initiator concentration to 0.2/2 Ru/SPS (mM/mM) significantly increased the polymerization rate ($p < 0.05$), resulting in the fabrication of hydrogels with sol fraction less than 30% within 0.5 min. The sol fraction values decreased as the exposure time increased and plateaued at approximately 15%. This minimal sol fraction value achieved was also comparable to gels cross-linked using Vis + 0.05 wt% LAP and UV + 0.05 wt% I2959 (Figure 2A). Furthermore, increasing the initiator concentration to 0.3/3 Ru/SPS (mM/mM) resulted in identical sol fraction profiles as 0.2/2 Ru/SPS (mM/mM). This result indicates that complete cross-linking of the Gel-MA macromers was achieved using 0.2/2 Ru/SPS

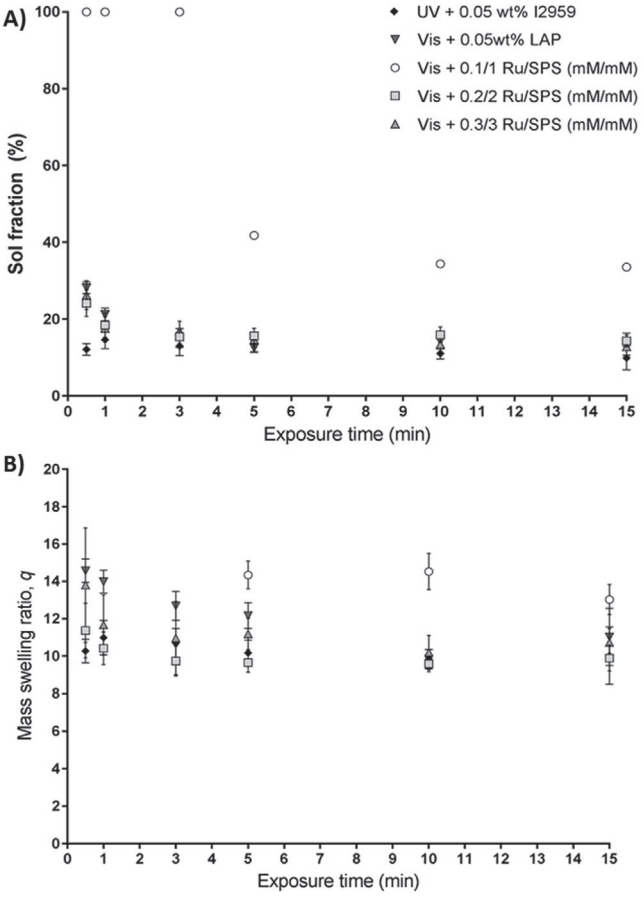

Figure 2. Physico-chemical properties of Gel-MA hydrogels fabricated using different concentrations of Ru/SPS as a function of exposure time: A) Sol fraction; B) mass swelling ratio, q. Gel-MA gels cross-linked using UV + 0.05 wt% I2959 and Vis + 0.05 wt% LAP were used as controls. Light intensities for both UV and visible (Vis) light were kept constant at 30 mW cm^{-2} for 15 min. Sol fraction values of 100% indicate no hydrogel formation.

(mM/mM). One major observation was that gels cross-linked using UV + 0.05 wt% I2959 had a faster polymerization rate, where the sol fraction value plateaued after 0.5 min of UV exposure.

Results obtained for the mass swelling ratio (q) complemented the sol–gel analysis, where a decrease in q was observed for longer exposure times (Figure 2B). Furthermore, samples with higher sol fraction possessed higher mass swelling ratios. Once again, increasing the initiator concentration from 0.2/2 Ru/SPS (mM/mM) to 0.3/3 Ru/SPS (mM/mM) did not show any significant differences in the mass swelling ratio ($p = 0.9680$), demonstrating that 0.2/2 Ru/SPS (mM/mM) was sufficient to completely cross-link the macromers.

3.1.2. Mechanical Testing of Gel-MA Hydrogels

It was observed that after 15 min of exposure at 30 mW cm^{-2}, Gel-MA hydrogels fabricated using 0.1/1 Ru/SPS (mM/mM) had a compressive modulus of 12.8 ± 1.7 kPa (**Figure 3**).

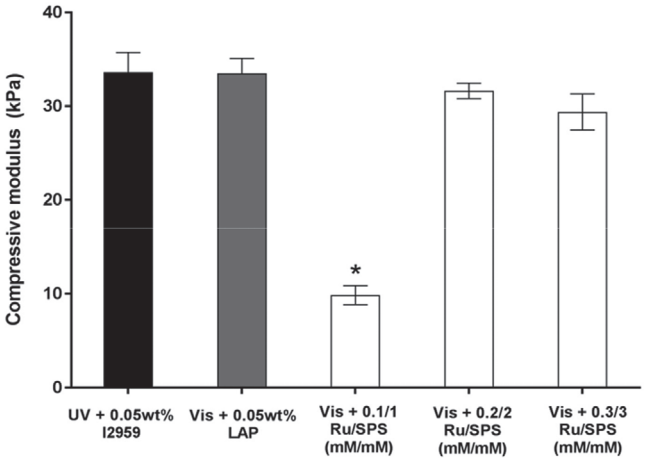

Figure 3. Compressive modulus of Gel-MA hydrogels fabricated using different concentrations of Ru/SPS. Light intensity and irradiation time were kept at 30 mW cm^{-2} and 15 min, respectively. Gel-MA gels cross-linked using UV + 0.05 wt% I2959 and Vis + 0.05 wt% LAP were used as controls. *Indicates significant difference to other columns ($p < 0.05$).

Increasing the initiator concentration to 0.2/2 Ru/SPS (mM/mM) resulted in hydrogels of significantly greater compressive modulus (31.6 ± 0.8 kPa, $p < 0.0001$), which were comparable to Gel-MA hydrogels fabricated using the conventional Vis + 0.05 wt% LAP (33.5 ± 1.6 kPa, $p = 0.5356$) and UV + 0.05 wt% I2959 (33.6 ± 2.1 kPa, $p = 0.4740$). However, no significant difference was observed when the initiator concentration was further increased to 0.3/3 Ru/SPS (mM/mM) (29.4 ± 1.9 kPa, $p = 0.3626$). Again, this result indicated that 0.2/2 Ru/SPS (mM/mM) was sufficient to completely cross-link the Gel-MA macromers, which led to the selection of this concentration for all further studies described herein.

3.2. HAC Encapsulation in Gel-MA Hydrogels

As the overall goal was to investigate the potential for the visible light cross-linking system to be used for 3D cell encapsulation in tissue engineering applications, expanded (passage 2) HACs were encapsulated into the 3D Gel-MA hydrogels. Live–dead fluorescence images following short- (1 day) and long-term (35 days) in vitro culture showed that the cell-laden gels fabricated using the UV + I2959, Vis + LAP, and Vis + Ru/SPS system demonstrated good viability and an abundance of live cells (Figure S1, Supporting Information). In a 3D environment, chondrocytes typically exhibit a rounded morphology as an indication of their chondrogenic phenotype.[45] For all time points, it was observed that in all the UV + I2959, Vis + LAP, and Vis + Ru/SPS system, the encapsulated cells were not only homogenously distributed, but also remained rounded (Figure S2, Supporting Information).

Total live/dead cell counts were used to evaluate viability of the encapsulated HACs. All systems demonstrated good cell viability over the 35-day culture period (>80%). Both the Vis + LAP and Vis + Ru/SPS system showed significantly higher cell viability than the UV + I2959 system for all three examined time points (**Figure 4**A). We also observed no significant differences between the two systems utilizing visible light photo-initiation in terms of cell viability across all time points. After longer-term culture for 35 days, HACs encapsulated using the UV + I2959 system showed a reduction in viability, whereas cell viability in both the Vis + LAP and Vis + Ru/SPS samples remained greater than 85%. These results suggest that the visible light photo-initiator system presents a more cyto-compatible environment as compared to the UV cross-linking system.

Furthermore, metabolic activity of each of the samples was examined in order to evaluate the biological function of encapsulated cells. It was observed that the Vis + Ru/SPS samples had significantly higher metabolic activity at 1 ($p = 0.0016$), 21 ($p = 0.0001$), and 35 days ($p < 0.0001$) compared to UV + I2959 (Figure 4B). Similarly, the Vis + LAP samples also showed statistically higher metabolic activity compared to gels cross-linked using UV + I2959 at 21 ($p = 0.0146$) and 35 days ($p < 0.0001$). These results indicate that although cells encapsulated in Gel-MA using the conventional UV + I2959 system exhibit favorable cell viability and metabolic activity throughout the culture period, the visible light system showed an improvement on both measures, which was likely due to the lower overall photo-toxicity, radical toxicity, and oxidative stress exerted on the cells.

To determine the ability of all UV + I2959, Vis + LAP, and Vis + Ru/SPS Gel-MA hydrogels to support biological function and extracellular matrix formation, the chondrogenic differentiation capacity of the HACs post encapsulation was examined in vitro. Figure 4D demonstrates that the encapsulated HACs were able to proliferate within the gels, regardless of which photo-initiation system was used, where an increase in DNA content was observed from 1 day to 35 days. However, no significant differences were observed across all three systems at every examined time point. In terms of tissue formation, there was a clear increase in total GAG content from 1 to 35 days in the UV + I2959 ($p < 0.0001$), Vis + LAP ($p < 0.001$), and Vis + Ru/SPS ($p < 0.0001$) constructs (Figure 4C). Both visible light systems resulted in significantly higher GAG content of samples, compared to those cross-linked with the UV + I2959 system at 21 and 35 days. In addition, HACs encapsulated using Vis + Ru/SPS secreted more GAGs in the hydrogels at 21 ($p = 0.0033$) and 35 days ($p < 0.0001$) after encapsulation, compared to the Vis + LAP cross-linked samples.

If we consider the re-differentiation capacity of cell encapsulated Gel-MA constructs, GAG/DNA in the UV + I2959, Vis + LAP, and Vis + Ru/SPS samples increased significantly from 1 to 35 days, indicating that these Gel-MA hydrogels are able to support chondrogenic differentiation of HACs (Figure 4E). However, most importantly, we observed that after 35 days in culture, constructs encapsulated using Vis + Ru/SPS had significantly higher GAG/DNA (14.2 ± 0.7 μg $μg^{-1}$) than in the Vis + LAP (12.5 ± 0.9 μg $μg^{-1}$, $p < 0.0001$) and UV + I2959 system (12.4 ± 0.4 μg $μg^{-1}$, $p < 0.0001$). Immunofluorescence analysis confirms that the encapsulated HACs secreted collagen type I, collagen type II, and aggrecan in the GelMA hydrogels, regardless of the applied photo-encapsulation system. Further quantitative analysis showed that there are no significant differences in terms of collagen type I and collagen type II production within the gels among all three photo-polymerization systems (**Figure 5**J,K). However, the total coverage area for aggrecan

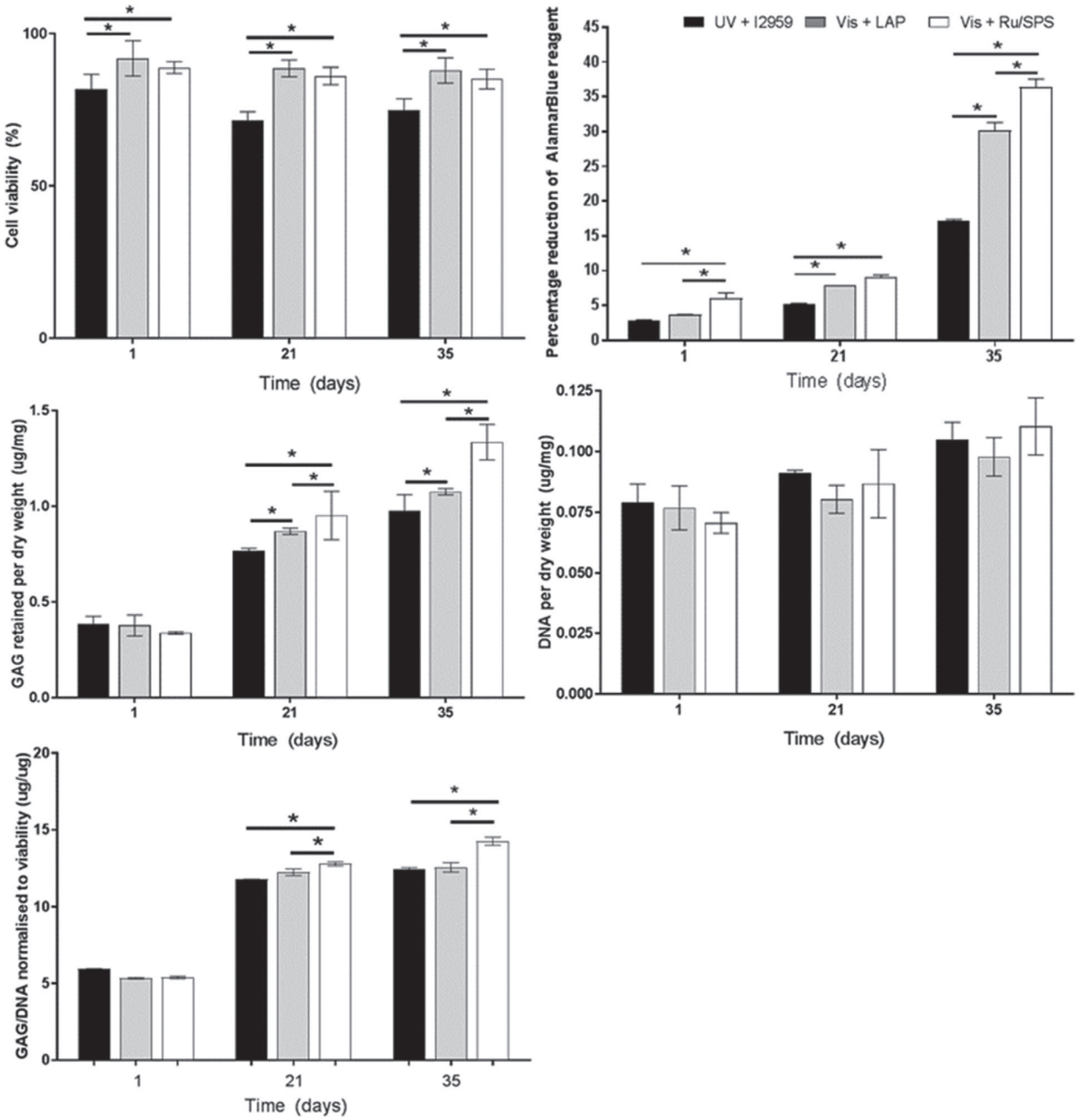

Figure 4. Encapsulation of HACs in Gel-MA hydrogels using UV + I2959, Vis + LAP, and Vis + Ru/SPS, at 1, 21, and 35 days in culture. A) Cell viability (%); B) metabolic activity reported as percentage reduction of Alamarblue reagent; C) GAG retained per dry weight (μg mg^{-1}); D) DNA per dry weight (μg mg^{-1}); C) GAG/DNA normalized to cell viability. *Significant differences between columns below each end of lines ($p < 0.05$).

was significantly higher in the Vis + Ru/SPS as compared to the UV + I2959 and Vis + LAP systems (Figure 5L) where a higher expression of aggrecan was stained in the pericellular regions of the HACs at day 35 in the Vis + Ru/SPS constructs (Figure 5G–I). Chondrogenic gene expressions at early culture time point (day 7) were evaluated to further study the effect of oxidative stress that is exerted on the cells during the photo-encapsulated process. We did observe that the gene expressions for collagen type II and aggrecan are indeed higher in the Vis + Ru/SPS systems (Figure 5M–O), further confirming our other observations that this photo-crosslinking system is more cell friendly and exerts less damage to the cells during the encapsulation process.

3.3. Light Penetration Depth Study

As the photo-polymerization processes can be applied to fabricate in vivo injectable hydrogels for tissue engineering applications, we further compared the effectiveness of the

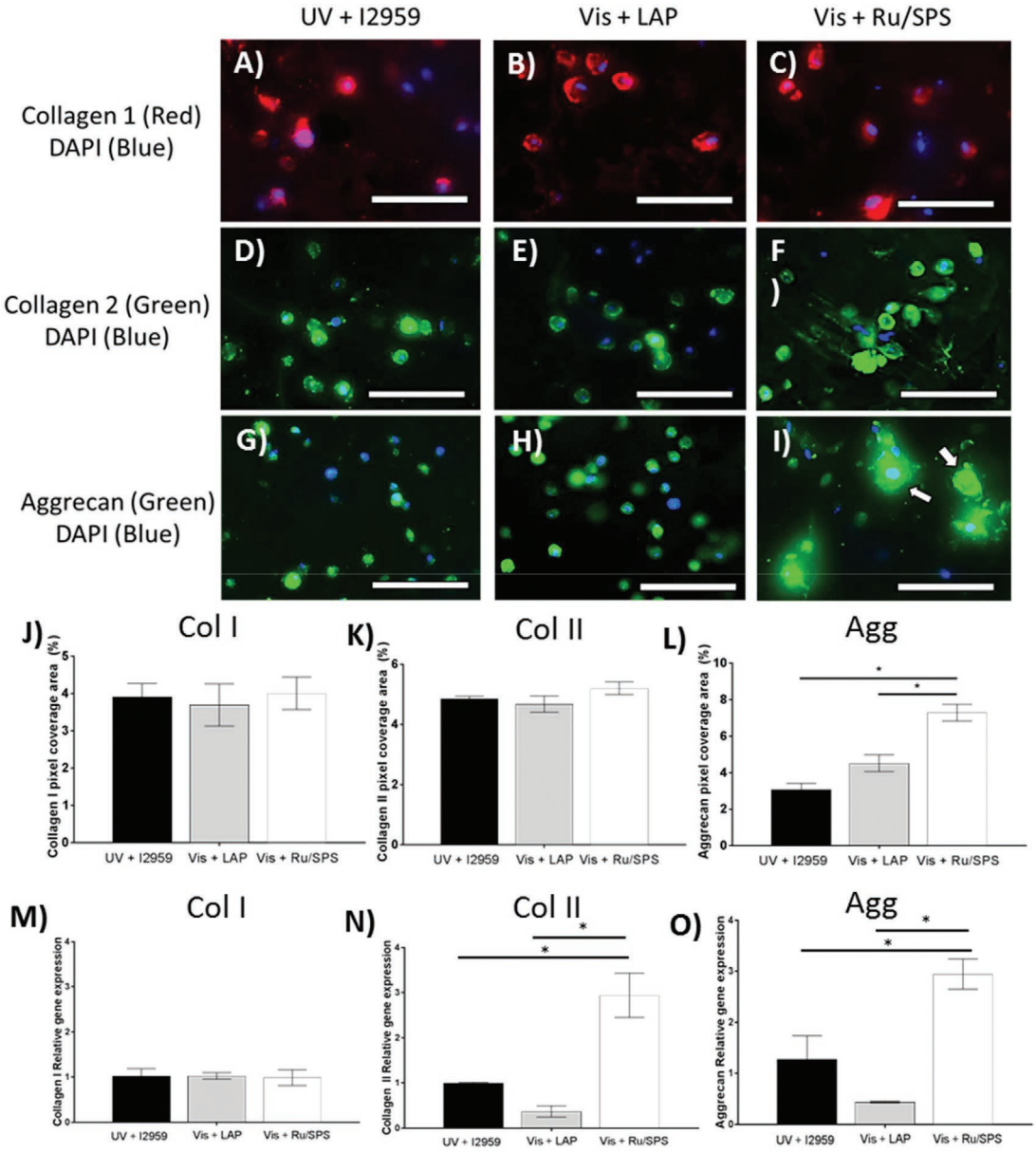

Figure 5. Immunofluorescence staining of HAC encapsulated in Gel-MA hydrogels using UV + I2959, Vis + LAP, or Vis + Ru/SPS after 35 days in culture: A–C) collagen type I; D–F) collagen type II; G–I) aggrecan. Pixel coverage area per panel for collagen I (J), collagen II (K), and aggrecan (L). Early relative gene expression after 7 days in culture: M) collagen I; N) collagen II; O) aggrecan. Scale bar = 100 µm. *Significant differences between columns below each end of lines ($p < 0.05$).

photo-polymerization systems for fabrication of thick hydrogel constructs (10 mm). One of the major advantages of using visible light is the better light penetration depth over UV that will be beneficial for transdermal polymerization or in situ cross-linking. As our cell encapsulation data suggested that the Vis + Ru/SPS is more superior over the Vis + LAP system in terms of HAC metabolic activity and re-differentiation capacity, we chose to only compare the Vis + Ru/SPS to the more conventional UV + I2959 for subsequent experiments. The UV + I2959 system demonstrated a limited penetration depth (6–8 mm), whereas Vis + Ru/SPS system was able to penetrate through and completely polymerize the entire 10 mm thick construct (**Figure 6**B). This observation was confirmed by mass loss data, where the Vis + Ru/SPS gels of different irradiation depths (i to v) had no significant difference in sol fraction values ($p > 0.98$). In contrast, for the UV + I2959 cross-linked samples, regions of the hydrogel farthest away from the irradiation source exhibited an increased sol fraction, with samples beyond 6 mm (regions iv and v) completely dissolving after 1 day (sol fraction = 100%). A similar trend was observed for the mass swelling ratios, where no significant difference was observed for the Vis + Ru/SPS cross-linked samples across all regions (i to v). However,

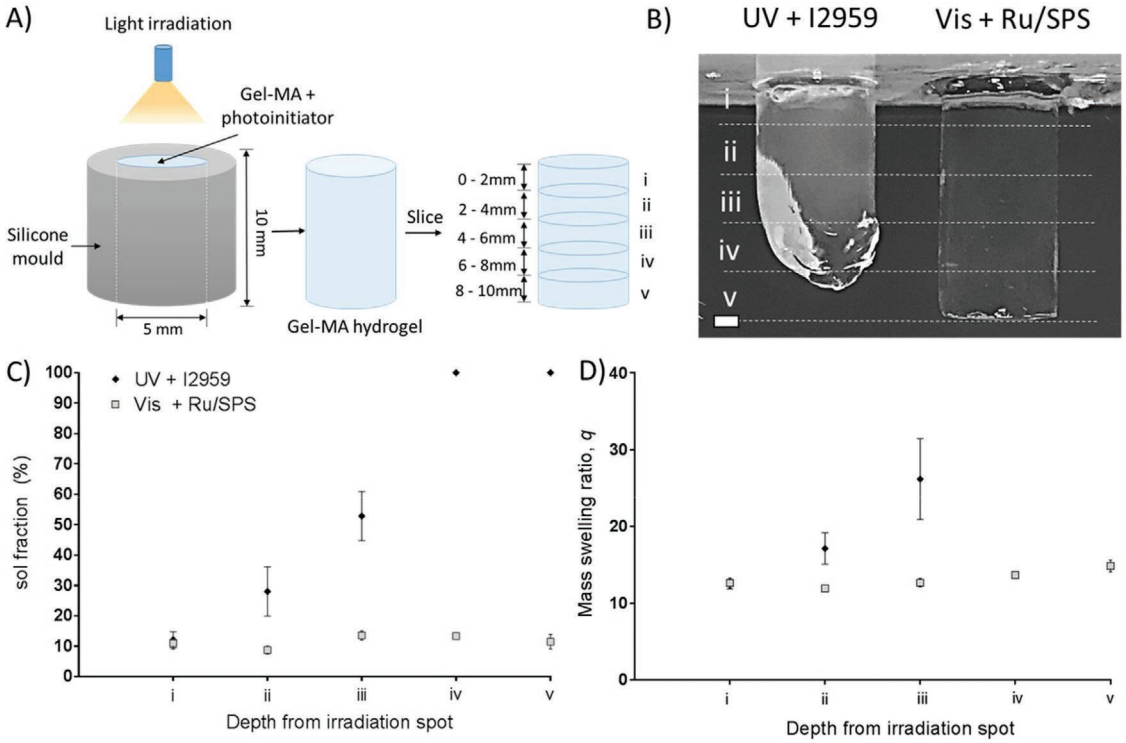

Figure 6. Fabrication of thick hydrogel constructs using both UV + I2959 and Vis + Ru/SPS systems: A) Schematic of light penetration depth setup; B) macroscopic images of Gel-MA constructs post photo-polymerization, scale bar = 1 mm; C) sol fraction values; D) mass swelling ratios of samples as per depth from irradiation spot.

gels cross-linked using the UV + I2959 had distinctly different swelling ratios at different depths from the irradiation source (Figure 6D). These results further indicated that UV light has limited penetration depth as well as being attenuated through the *z*-axis during photo-crosslinking, resulting in varying cross-linking density with depth within the hydrogel.

We further extended our studies to evaluate cell viability within the samples at different depths from the irradiation source (**Figure 7**). Interestingly, we observed an increase in cell viability at increasing depths for the UV cross-linked samples, where cells in the middle regions (iii, 4–6 mm from the irradiation source) had significantly higher viability ($p < 0.0001$) than those cells closer to the light source (i, <2 mm from the irradiation source). This data concur with our previous mass loss results (Figure 6C), where UV light was likely being attenuated through the *z*-axis, with cells at different irradiation depths being subjected to different UV light intensity. In contrast, no significant differences in cell viability were observed for the Vis + Ru/SPS samples throughout the full 10 mm depth of the construct (regions i–v)

3.4. Transdermal Polymerization Study and In Vivo Subcutaneous Implantation

One of the major advantages of having a greater light penetration depth is the potential use of this visible light photo-crosslinking system for transdermal polymerization. We evaluated the possibility to fabricate hydrogels transdermally using murine skin (0.5 mm) as a model (**Figure 8**A), and observed that UV light had limited transmission through skin resulting in the formation of a weak gel that was completely dissolved after 1 day (100% sol fraction, Figure 8B). In contrast, hydrogels were successfully cross-linked using visible light transmitted through the murine skin, with no statistical difference in sol fraction and swelling ratio to the control (Figure 8B). In vivo studies showed that after 14 days of subcutaneous implantation, there was limited cell infiltration into the hydrogels fabricated using both the UV + I2959 and Vis + Ru/SPS system. No significant differences were observed in terms of the host response to the gels fabricated using both these systems, again suggesting that there were no distinct differences in the physico-chemical and mechanical properties of hydrogels cross-linked using either UV + I2959 or Vis + Ru/SPS, and is in agreement with our in vitro data.

4. Discussion

In this study, we demonstrated that the optimal irradiation conditions to fabricate Gel-MA hydrogels consisted of a visible light intensity of 30 mW cm^{-2}, photo-initiator concentration of 0.2/2 Ru/SPS (mM), and at least 3 min of exposure time. However more importantly, it should be recognized that the Ru/SPS concentration required to fully photo-crosslink Gel-MA hydrogels in this study was ten times lower than the initiator concentrations reported to date in the literature to cross-link other polymers via their phenol moieties.[4,46,47] This difference in initiator

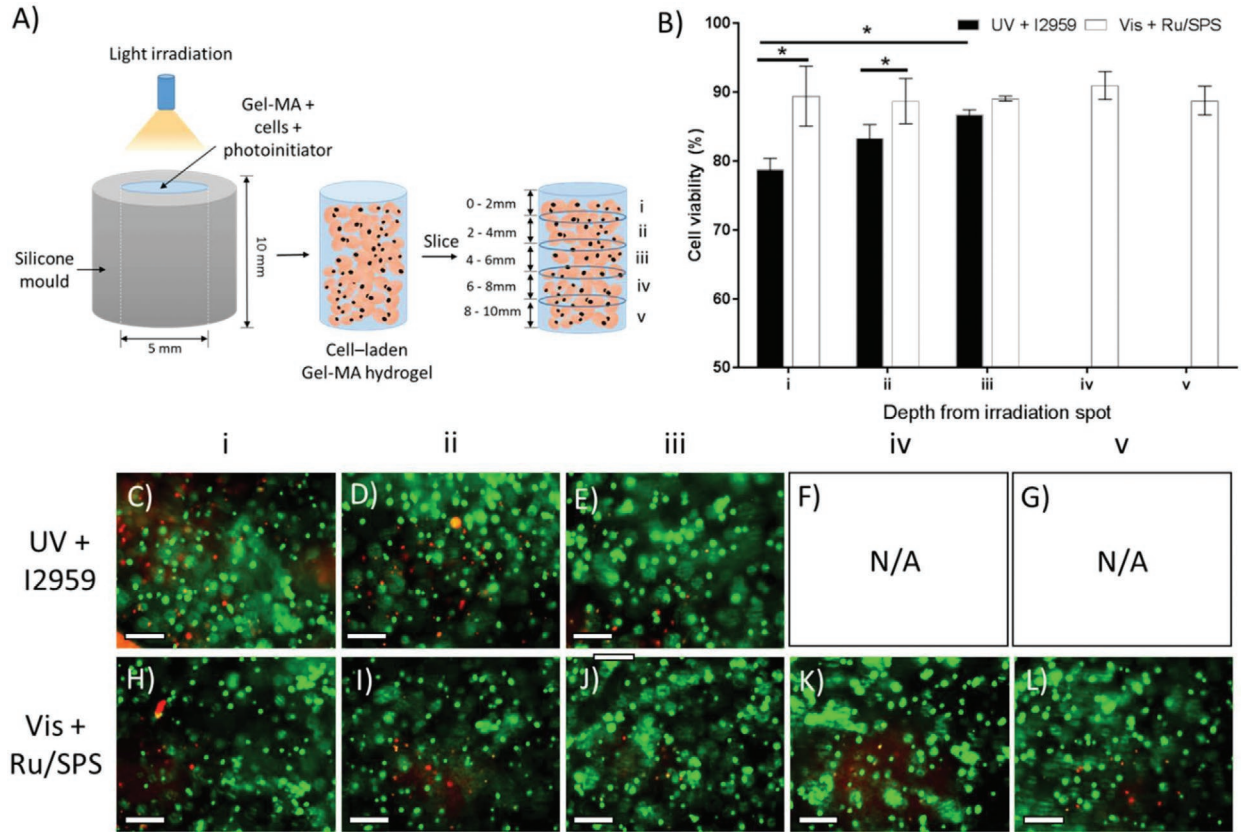

Figure 7. Fabrication of thick cell-laden constructs using both UV + I2959 and Vis + Ru/SPS systems: A) Schematic of light penetration depth setup; B) cell viability at different depths from the light irradiation spot. Live dead images of UV + I2959 cross-linked samples (C–G) for different irradiation depths i, ii, iii, iv, and v, respectively; scale bar = 100 µm. Images (F) and (G) were not available due to the gels completely dissolved after 1 day in culture. Live dead images of Vis + Ru/SPS cross-linked samples (H–L) for different irradiation depths i, ii, iii, iv, and v, respectively; scale bar = 100 µm.

concentrations between Gel-MA and the other phenolated polymers, such as gelatin, fibrinogen, resilin, and tyraminated PVA, may likely be due to the reactivity of different functional groups, as well as different initiator components that are responsible for cross-linking. During the photo-polymerization process, Ru^{2+} is photo-excited to Ru^{3+} by donating electrons to SPS.[35,48] For other phenolated polymeric systems, Ru^{3+} is responsible for the cross-link formation. However, in our case, the sulfate radicals which are products from the dissociation of SPS are responsible for reacting with methacryloyl groups on Gel-MA to form covalent cross-links. As the reaction between the sulfate radicals and the methacryloyl groups is more effective than the reaction between the Ru^{3+} and phenol groups, less Ru/SPS is therefore required to cross-link the Gel-MA hydrogels. On the other hand, however, the Ru^{3+} component may contribute to cross-linking the phenol groups present in the gelatin backbone concurrently.

The sol fraction (10–15%), mass swelling ratio q (9–10), and compressive moduli (≈20 kPa) obtained for Vis + 0.2/2 Ru/SPS (mM/mM) Gel-MA hydrogels in this study are comparable to properties obtained for Gel-MA gels fabricated using the UV + I2959 and Vis + LAP systems.[49,50] This result indicates that the visible light system is capable of fabricating Gel-MA hydrogels of equivalent physico-mechanical properties to the other more conventional and widely adopted photo-initiated polymerization system. Although we did observe that the UV + I2959 system had a faster cross-linking rate compared to both the Vis + LAP and Vis + Ru/SPS systems, the mass loss and swelling studies were conducted in an ideal environment without taking oxygen inhibition and light penetration depth into account, where the macromer was irradiated while sandwiched between a glass slide and cover slip, and is not an accurate representation of the downstream application. Moreover, in addition to Gel-MA hydrogels alone, we have successfully employed this visible light system to other polymers including heparin, hyaluronic acid, poly(vinyl alcohol), and gellan gum, all of which were functionalized with unsaturated vinyl moieties, such as methacryloyl or allyl groups.[36,38,51] Taking these factors into account, our work suggests that both synthetic and biological polymers modified with functional vinyl moieties can be cross-linked through different chemistries such as chain-growth methacryloyl or step-growth thiol–ene photo-click polymerization, using Vis + Ru/SPS.

As expected, encapsulated cells had high cell viability (>80%) after 1 day for both photo-initiator systems. This result is comparable to a previous study reported by Schuurman et al. where after 1 day, the viability of equine articular chondrocytes encapsulated in 10 wt% Gel-MA gels cross-linked using UV + I2959 was approximately 83%.[52] Nichol et al. also showed that fibroblasts encapsulated in 10 wt% Gel-MA gels had viability of

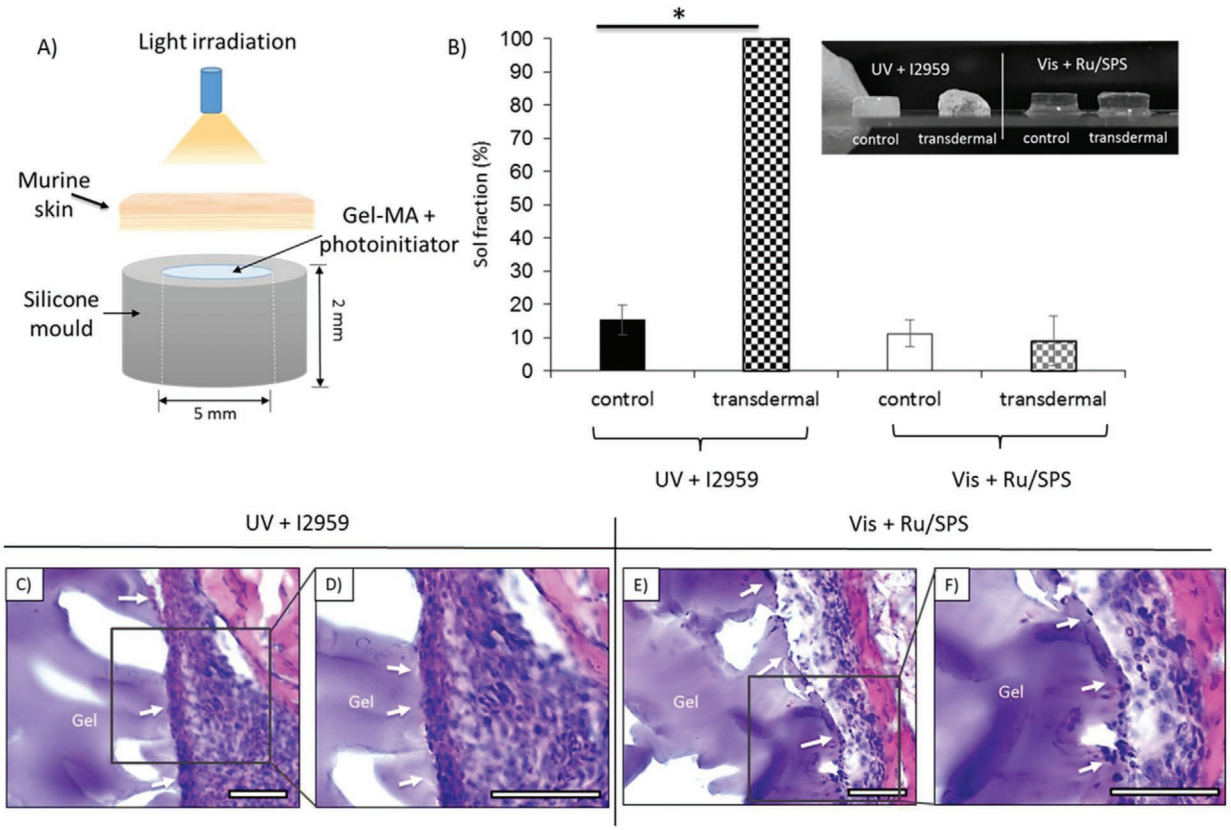

Figure 8. Transdermal polymerization of Gel-MA constructs using both UV + I2959 and Vis + Ru/SPS systems: Schematic (A) and sol fraction (B) of Gel-MA hydrogels photo-crosslinked using light transmitted through murine skin; immunohistochemical staining (H&E) of Gel-MA hydrogels fabricated using UV + I2959 (C,D) and Vis + Ru/SPS (E,F) post 14 days implanted subcutaneously. White arrows pointing to hydrogel and tissue interface. Scale bar = 100 µm.

82% after UV polymerization.[49] In this study, applying either the Vis + LAP or Vis + Ru/SPS system resulted in cell-laden hydrogel constructs with an improved cell viability and significantly higher metabolic activity than UV gels. We believe that this result might be due to the negative effect of UV irradiation to the cells, which has been shown to cause genomic instability of cells.[38,53,54] Previous work from Greene et al. describes that hepatocytes photo-encapsulated in gelatin–norbornene gels using visible light + eosin-Y had significantly higher metabolic activity compared to their UV counterparts.[14] Caliari et al. also showed that UV irradiation significantly reduced the cell viability of hepatic stellate cells when compared to visible light for encapsulation in methacrylated hyaluronic acid hydrogels.[55] Furthermore, UV is known to react with oxygen in the environment, forming ROS such as superoxide radical ($O_2^{\cdot-}$), hydroxyl radical ($OH^{\cdot}$), singlet oxygen ($^1O_2$), and ozone (O_3), which can oxidize the lipid bilayer of cells.[54,56,57] This lipid peroxidation may disrupt the cell membrane integrity and permeability, which can lead to upregulation of tissue degrading enzymes and generation of toxic products.[54,57] The chondrogenic differentiation study showed that GAG content and re-differentiation capacity (GAG/DNA) of HACs were significantly higher in the Vis + Ru/SPS samples than their Vis + LAP and UV + I2959 counterparts after long-term 35 day culture. As both LAP and Ru/SPS require visible light for photo-initiation, the difference observed in cell viability, metabolic activity, and re-differentiation capacity might be due to the diverse radical generation mechanism. We hypothesize that the Ru + SPS system has a slower but more sustained radical generation rate being a non-cleavage type 2 photo-initiator that undergoes a self-recycling mechanism (Figure 1).[35,39,48,58] It has been previously reported that this ability to re-initiate polymerization allows type 2 photo-initiators to be less affected by oxygen inhibition.[58] Further covalent incorporation of chondrogenic factors or growth factor–binding peptides within Vis + Ru/SPS Gel-MA hydrogels (such as TGF-ß1, hyaluronic acid, heparin) would likely further enhance this chondrogenic niche.[12,59]

The clinical relevance of these visible light initiating systems are particularly appealing for cell delivery or as space-fillers post augmentation, where in situ photo-curing typically requires high light intensity to minimize both oxygen inhibition and light attenuation. We demonstrated that the UV + I2959 system has a limited light penetration depth and can be attenuated during photo-crosslinking of constructs greater than 2 mm in thickness. Although a maximum penetration depth of 6 mm could be achieved with UV, variations in physical properties (sol fraction and mass swelling ratio) and cell viability were detected, indicating an inhomogeneous and sub-optimal

cross-linking density throughout the construct. Our findings correlate to previous studies which also highlighted the limited penetration depth of UV light in either photo-curing of dental resin,[60] photo-responsive polymers,[61,62] or transdermal photo-polymerization.[23] The Vis + Ru/SPS system showed an added advantage in having enhanced penetration depth with homogenous cross-linking density and cell viability throughout a 10-mm thick construct. Furthermore, we have also reported that the Vis + Ru/SPS system is less susceptible to oxygen inhibition compared to the UV + I2959 system, allowing fabrication of large 3D bioprinted constructs with good shape fidelity.[39] In a transdermal polymerization setup, we observed that a visible light intensity of 30 mW cm^{-2} was enough to transmit through the murine skin and enable photo-crosslinking of the Gel-MA + 0.2/2 (mM/mM) Ru/SPS macromer. In contrast, using the same UV intensity and 0.05 wt% I2959 did not result in successful hydrogel fabrication, highlighting the limited skin penetration and transmittance of light in the UV range. Lin et al. previously showed that a combination of higher UV intensity (40 mW cm^{-2}) and I2959 concentration (0.5 wt%) was indeed able to facilitate transdermal polymerization of Gel-MA hydrogels.[63] However, we showed that the Vis + Ru/SPS system is significantly more efficient where lower visible light intensity and Ru/SPS concentrations were sufficient to transdermally fabricate hydrogels of similar quality to the controls. Although the murine skin model (0.5 mm) used in this study is thinner, it does consist of three distinctive layers (epidermis, dermis, and hypodermis) similarly to human skin (1–2 mm). The cytotoxicity of the transition metal Ru might raise some concerns for use in clinical applications. Therefore, we conducted a cell growth inhibition assay to assess the toxicity of Ru in accordance to the ISO10993 standard. We observed that the concentration of Ru (0.2 mM) used in this study is below the accepted cytotoxicity threshold (<30%, Figure S1, Supporting Information). This result is in agreement with a previous study conducted by Elvin et al., where even a concentration as high as 1 mM of Ru was not cytotoxic.[10] In the same study, Elvin et al. also showed that gelatin-tyramines were fabricated into tissue sealants using 1/20 Ru/SPS (mM/mM) and showed minimal inflammatory response and no adverse cytotoxic reactions based on histological analysis.[10] Similarly, our in vivo subcutaneous study also displayed that the Gel-MA hydrogels fabricated using Vis + Ru/SPS showed no significant difference in host tissue reaction in comparison to the UV + I2959 counterparts (Figure 8C–F).

We believe that adopting the Vis + Ru/SPS system offers advantages over the UV irradiation system with respect to not only promoting cell viability and function within in situ photocured hydrogels or 3D constructs, but importantly to host cells in surrounding healthy issue that would also be exposed to high light intensity, particularly during the photo-polymerization of thick or large constructs. Furthermore, we purport that the applicability of the Vis + Ru/SPS system may be of particular benefit over Vis + LAP and UV + I2959 systems in the field of biofabrication or 3D bioprinting of thick, cell-laden constructs, where again, high light intensity or high photo-initiator concentration are generally necessary to maintain shape fidelity of biofabricated constructs as well as obtain maximum cell survival.[39]

5. Conclusions

We have demonstrated and optimized the use of the visible light photo-initiators (Ru/SPS) to fabricate Gel-MA hydrogels. The fabricated gels offered similar physico-chemical and mechanical properties compared to those cross-linked using conventionally adopted UV + I2959 photo-initiator system. HACs encapsulated in visible light polymerized gels demonstrated superior cell viability and metabolic activity, as well as greater GAG content and re-differentiation capacity (GAG/DNA) as compared to UV cross-linked Gel-MA hydrogels. Furthermore, the enhanced penetration depth observed for the visible light system offers added benefits for in situ photo-curing applications and fabrication of thick hydrogel constructs. This study highlights the potential of this Vis + Ru/SPS system for the fabrication of Gel-MA gels for not only cartilage engineering, but also other tissue engineering applications including cell delivery and in-situ photo-curing.

Supporting Information

Supporting Information is available from the Wiley Online Library or from the author.

Acknowledgements

The authors wish to acknowledge Dr. Ben Schon for his scientific input and his involvement in the subcutaneous implantation study. The authors also wish to acknowledge the funding support from the Royal Society of New Zealand Rutherford Discovery Fellowship (RDF-UOO1204; TW), Health Research Council of New Zealand Emerging Researcher First Grant and Sir Charles Hercus Fellow (HRC 15/483 and 19/135; KL), the EU/FP7 "skelGEN" consortium under grant agreement no. 318553, and the Dutch Arthritis Foundation (LLP-12; JM).

Conflict of Interest

The authors declare no conflict of interest.

Keywords

cell encapsulation, gelatin-methacryloyl (Gel-MA), hydrogels, light penetration depth, transdermal crosslinking, visible light

Received: March 28, 2019
Published online: April 26, 2019

[1] K. S. Lim, J. J. Roberts, M.-H. Alves, L. A. Poole-Warren, P. J. Martens, *J. Appl. Polym. Sci.* **2015**, *132*, 42142.
[2] E. H. Nafea, L. A. Poole-Warren, P. J. Martens, *J. Biomater. Sci., Polym. Ed.* **2014**, *25*, 1771.
[3] B. S. Schon, G. J. Hooper, T. B. F. Woodfield, *Ann. Biomed. Eng.* **2017**, *45*, 100.
[4] K. S. Lim, M. H. Alves, L. A. Poole-Warren, P. J. Martens, *Biomaterials* **2013**, *34*, 7907.
[5] S. Bryant, G. Nicodemus, I. Villanueva, *Pharm. Res.* **2008**, *25*, 2379.

[6] A. I. Van Den Bulcke, B. Bogdanov, N. De Rooze, E. H. Schacht, M. Cornelissen, H. Berghmans, *Biomacromolecules* **2000**, *1*, 31.
[7] T. Manabe, H. Okino, M. Tanaka, T. Matsuda, *Biomaterials* **2004**, *25*, 5867.
[8] T. Vuocolo, R. Haddad, G. A. Edwards, R. E. Lyons, N. E. Liyou, J. A. Werkmeister, J. A. M. Ramshaw, C. M. Elvin, *J. Gastrointest. Surg.* **2012**, *16*, 744.
[9] A. Hoshikawa, Y. Nakayama, T. Matsuda, H. Oda, K. Nakamura, K. Mabuchi, *Tissue Eng.* **2006**, *12*, 2333.
[10] C. M. Elvin, T. Vuocolo, A. G. Brownlee, L. Sando, M. G. Huson, N. E. Liyou, P. R. Stockwell, R. E. Lyons, M. Kim, G. A. Edwards, G. Johnson, G. A. McFarland, J. A. M. Ramshaw, J. A. Werkmeister, *Biomaterials* **2010**, *31*, 8323.
[11] F. P. W. Melchels, W. J. A. Dhert, D. W. Hutmacher, J. Malda, *J. Mater. Chem. B* **2014**, *2*, 2282.
[12] G. C. J. Brown, K. S. Lim, B. L. Farrugia, G. J. Hooper, T. B. F. Woodfield, *Macromol. Biosci.* **2017**, *17*, 1700158.
[13] B. J. Klotz, D. Gawlitta, A. J. W. P. Rosenberg, J. Malda, F. P. W. Melchels, *Trends Biotechnol.* **2016**, *34*, 394.
[14] T. Greene, T. Lin, M. A. Ourania, C. Lin, *J. Appl. Polym. Sci.* **2016**, *134*, 44585.
[15] S. J. Bryant, C. R. Nuttelman, K. S. Anseth, *J. Biomater. Sci., Polym. Ed.* **2000**, *11*, 439.
[16] F. R. de Gruijl, H. J. van Kranen, L. H. F. Mullenders, *J. Photochem. Photobiol. B* **2001**, *63*, 19.
[17] J. Dahle, E. Kvam, *Cancer Res.* **2003**, *63*, 1464.
[18] J. Dahle, E. Kvam, T. Stokke, *J. Carcinog.* **2005**, *4*, 11.
[19] R. Lavker, K. Kaidbey, *J. Invest. Dermatol.* **1997**, *108*, 17.
[20] A. Urushibara, S. Kodama, A. Yokoya, *Mut. Res., Genet. Toxicol. Environ. Mutagen.* **2014**, *766*, 29.
[21] J. G. Peak, M. J. Peak, *Mut. Res. Fundam. Mol. Mech. Mutagen.* **1991**, *246*, 187.
[22] M. S. Cooke, M. D. Evans, M. Dizdaroglu, J. Lunec, *FASEB J.* **2003**, *17*, 1195.
[23] J. Elisseeff, K. Anseth, D. Sims, W. McIntosh, M. Randolph, R. Langer, *Proc. Natl. Acad. Sci. USA* **1999**, *96*, 3104.
[24] J. Hu, Y. Hou, H. Park, B. Choi, S. Hou, A. Chung, M. Lee, *Acta Biomater.* **2012**, *8*, 1730.
[25] J. Jakubiak, X. Allonas, P. Fouassier J, A. Sionkowska, E. Andrzejewska, L. Å. Linden, J. F. Rabek, *Polymer* **2003**, *44*, 5219.
[26] T. Mazaki, Y. Shiozaki, K. Yamane, A. Yoshida, M. Nakamura, Y. Yoshida, D. Zhou, T. Kitajima, M. Tanaka, Y. Ito, *Sci. Rep.* **2015**, *4*, 4457.
[27] B. D. Fairbanks, M. P. Schwartz, C. N. Bowman, K. S. Anseth, *Biomaterials* **2009**, *30*, 6702.
[28] H. Lin, D. Zhang, P. G. Alexander, G. Yang, J. Tan, A. W.-M. Cheng, R. S. Tuan, *Biomaterials* **2013**, *34*, 331.
[29] H. Shih, C. C. Lin, *Macromol. Rapid Commun.* **2013**, *34*, 269.
[30] C. S. Bahney, T. J. Lujan, C. W. Hsu, M. Bottlang, J. L. West, B. Johnstone, *Eur. Cells Mater.* **2011**, *22*, 43.
[31] E. Pelin, S. Fidan, B. Tugba, K. Seda, *Macromol. Biosci.* **2018**, *18*, 1700369.
[32] I. Noshadi, B. W. Walker, R. Portillo-Lara, E. Shirzaei Sani, N. Gomes, M. R. Aziziyan, N. Annabi, *Sci. Rep.* **2017**, *7*, 4345.
[33] N. Annabi, D. Rana, E. Shirzaei Sani, R. Portillo-Lara, J. L. Gifford, M. M. Fares, S. M. Mithieux, A. S. Weiss, *Biomaterials* **2017**, *139*, 229.
[34] K. S. Lim, Y. Ramaswamy, J. J. Roberts, M.-H. Alves, L. A. Poole-Warren, P. J. Martens, *Macromol. Biosci.* **2015**, *15*, 1423.
[35] D. A. Fancy, C. Denison, K. Kim, Y. Xie, T. Holdeman, F. Amini, T. Kodadek, *Chem. Biol.* **2000**, *7*, 697.
[36] K. S. Lim, R. Levato, P. F. Costa, M. D. Castilho, C. R. Alcala-Orozco, K. M. A. van Dorenmalen, F. P. W. Melchels, D. Gawlitta, G. J. Hooper, J. Malda, T. B. F. Woodfield, *Biofabrication* **2018**, *10*, 034101.
[37] P. Muller, K. Brettel, *Photochem. Photobiol. Sci.* **2012**, *11*, 632.
[38] S. Bertlein, G. C. J. Brown, K. S. Lim, T. Jungst, T. Boeck, T. Blunk, J. Tessmar, G. J. Hooper, T. B. F. Woodfield, J. Groll, *Adv. Mater.* **2017**, *29*, 1703404.
[39] K. S. Lim, B. S. Schon, N. V. Mekhileri, G. C. J. Brown, C. M. Chia, S. Prabakar, G. J. Hooper, T. B. F. Woodfield, *ACS Biomater. Sci. Eng.* **2016**, *2*, 1752.
[40] T. B. F. Woodfield, C. A. Van Blitterswijk, J. De Wijn, T. J. Sims, A. P. Hollander, J. Riesle, *Tissue Eng.* **2005**, *11*, 1297.
[41] C. M. Elvin, A. G. Brownlee, M. G. Huson, T. A. Tebb, M. Kim, R. E. Lyons, T. Vuocolo, N. E. Liyou, T. C. Hughes, J. A. M. Ramshaw, J. A. Werkmeister, *Biomaterials* **2009**, *30*, 2059.
[42] C. M. Elvin, A. G. Carr, M. G. Huson, J. M. Maxwell, R. D. Pearson, T. Vuocolo, N. E. Liyou, D. C. C. Wong, D. J. Merritt, N. E. Dixon, *Nature* **2005**, *437*, 999.
[43] P. Martens, K. S. Anseth, *Polymer* **2000**, *41*, 7715.
[44] J. J. Roberts, P. Naudiyal, K. S. Lim, L. A. Poole-Warren, P. J. Martens, *Biomater. Res.* **2016**, *20*.
[45] K. Schrobback, T. J. Klein, T. B. Woodfield, *Tissue Eng., Part A* **2015**, *21*, 1785.
[46] L. Sando, S. Danon, A. G. Brownlee, R. J. McCulloch, J. A. M. Ramshaw, C. M. Elvin, J. A. Werkmeister, *J. Tissue Eng. Regener. Med.* **2011**, *5*, 337.
[47] L. Sando, M. Kim, M. L. Colgrave, J. A. M. Ramshaw, J. A. Werkmeister, C. M. Elvin, *J. Biomed. Mater. Res., Part A* **2010**, *95A*, 901.
[48] D. A. Fancy, T. Kodadek, *Proc. Natl. Acad. Sci. USA* **1999**, *96*, 6020.
[49] J. W. Nichol, S. T. Koshy, H. Bae, C. M. Hwang, *Biomaterials* **2010**, *31*, 5536.
[50] W. Schuurman, V. Khristov, M. W. Pot, P. R. van Weeren, W. J. Dhert, J. Malda, *Biofabrication* **2011**, *3*, 021001.
[51] J. Parrish, K. S. Lim, K. Baer, G. J. Hooper, T. Woodfield, *Lab Chip* **2018**, *18*, 2757.
[52] W. Schuurman, P. A. Levett, M. W. Pot, P. R. van Weeren, W. J. A. Dhert, D. W. Hutmacher, F. P. W. Melchels, T. J. Klein, J. Malda, *Macromol. Biosci.* **2013**, *13*, 551.
[53] G. J. Clydesdale, G. W. Dandie, H. K. Muller, *Immunol. Cell Biol.* **2001**, *79*, 547.
[54] B. Halliwell, S. Chirico, *Am. J. Clin. Nutr.* **1993**, *57*, 715S.
[55] S. R. Caliari, M. Perepelyuk, B. D. Cosgrove, S. J. Tsai, G. Y. Lee, R. L. Mauck, R. G. Wells, J. A. Burdick, *Sci. Rep.* **2016**, *6*, 21387.
[56] H. S. El-Beltagi, H. I. Mohamed, *Not. Bot. Horti Agrobot. Cluj-Napoca* **2013**, *41*, 44.
[57] M. E. Greenberg, X.-M. Li, B. G. Gugiu, X. Gu, J. Qin, R. G. Salomon, S. L. Hazen, *J. Biol. Chem.* **2008**, *283*, 2385.
[58] K. Kaastrup, H. D. Sikes, *Chem. Soc. Rev.* **2016**, *45*, 532.
[59] P. A. Levett, F. P. W. Melchels, K. Schrobback, D. W. Hutmacher, J. Malda, T. J. Klein, *Acta Biomater.* **2014**, *10*, 214.
[60] A. Santini, I. T. Gallegos, C. M. Felix, *Prim. Dent. J.* **2013**, *2*, 30.
[61] A. M. Kloxin, M. W. Tibbitt, A. M. Kasko, J. A. Fairbairn, K. S. Anseth, *Adv. Mater.* **2010**, *22*, 61.
[62] D. Wang, M. Wagner, H.-J. Butt, S. Wu, *Soft Matter* **2015**, *11*, 7656.
[63] R.-Z. Lin, Y.-C. Chen, R. Moreno-Luna, A. Khademhosseini, J. M. Melero-Martin, *Biomaterials* **2013**, *34*, 6785.